The puzzle of a comprehensive picture of drift phenomenon in chalchogenide alloys

Paolo Fantini
Micron, Process R&D, Agrate Brianza (MB) - Italy, pfantini@micron.com

ABSTRACT

In a phase change memory the device resistance corresponding to the amorphous phase monotonically increases with time after the reset programming operation. This phenomenon, called drift, affects the stability of the high resistive state, namely the reset state. In this work, the prismatic picture of the experimental findings on drift oriented to have a unified interpretation will be reported. The debate on the physical description of structural relaxation (SR) phenomena leading to the drift of the current will be discussed.

Key words: Phase Change Memory, drift, Structural Relaxations, GST.

1. INTRODUCTION

Among today Non-Volatile Memory technologies, Phase-Change Memory (PCM) is one of the most attracting, featuring very fast programming, outstanding scalability perspectives, and very good retention properties [1]. The PCM memory technology exploits the ability of some chalcogenide alloys to perform reversible and fast amorphous/crystalline phase transitions through the application of suitable electrical stimuli. In particular, the PCM cell is programmed through a current pulse promoting the phase transition after melting of the active region of the chalcogenide-based material, typically a $Ge_2Sb_2Te_5$ (GST) film. The subsequent cooling from the Joule heating induced molten phase leaves the cell in the amorphous (reset) or crystalline (set) state, depending on the fast or slow trailing edge of the current pulse, respectively. The strong electric contrast between the amorphous and crystalline phase allows discriminating the logic state of the PCM. In fact, the disordered amorphous phase is insulating, while the crystalline one shows conducting behavior. Moreover, when the phase-change material is quenched in the amorphous phase by means of the reset programming operation, the cell current I decreases with time t according to the following power law [2]:

$$I(t) = I_0 \left(\frac{t}{t_0} \right)^{-\nu} \tag{1}$$

where I_0 is the current at a reference time t_0 and ν is the drift exponent, usually around 0.1 at room temperature and low field biasing. This tendency of the current to decrease with time after the amorphous phase programming is called *drift* and needs to be fully understood and controlled to ensure the necessary reliability of high-density PCM arrays.
Controversial theories have been proposed in order to explain the origin of drift in the amorphous phase of chalcogenide materials: A. Pirovano et al. [3] proposed that defects increase over time shifts the Fermi level of the amorphous network; I.V. Karpov et al. [4] indicated the release of the compressive stress in the amorphous region as physical origin of drift; while D. Ielmini et al. [5] suggested that structural relaxation (SR) phenomena occur in the chalcogenide-based amorphous network, having many metastable configurational states that compete in energy, thus they evolve over

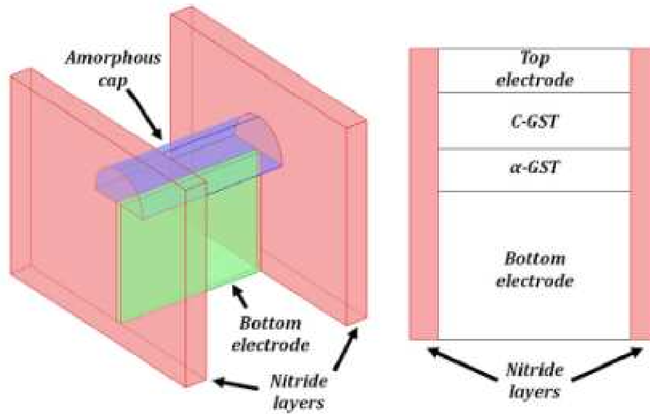

FIG. 2. (Color online) Schematic layout (left) and cross section (right) of a PCM device, indicating the amorphous cap, the bottom electrode, or BE, and the nitride stressor layers.

time to reach a more stable thermodynamic state as observed for other amorphous semiconductors and metallic glasses [6-9].

2. THE FIRST PIECE: MECHANICAL STRESS

In this scenario, we recently demonstrated that the mechanical stress that is developed by the denser crystalline phase surrounding the amorphous region in a mushroom type PCM cell cannot be invoked as the driving force of the drift phenomenon, since drift is observed also in stress-free α-GST films [10].To further investigate the role of mechanical stress above the limit of 50 MPa, which was the maximum achievable by our mechanical bending setup without breaking the sample, we studied resistance drift in PCM devices where a local compressive/tensile stress was added in the active region through dedicated process steps. Stress levels of few hundreds of MPa can be developed and engineered in MOS transistor where the stress can result in beneficial effects, such as improved dopant diffusion and carrier mobility [11]. In the PCM cell, a mechanical stress was induced by changing the process of fabricating the silicon-nitride (SiN_x) insulating layers between adjacent cells, as shown in the illustrative cell layout in Fig. 1. The different stress levels in the GST film were achieved changing the RF power during the plasma-enhanced chemical vapor deposition of the nitride films. An increase of the RF power may in fact lead to a higher surface temperature and/or a shallow implantation of ions, thus inducing a larger compressive stress. Two different stress levels in the nitride layers were thus obtained, corresponding to an average compressive stress of 750 MPa and 900 MPa in the GST amorphized region, as obtained from FEM calculations considering both the volume expansion in the amorphous region and the pre-existent stress due to the nitride layers. Fig. 2a shows

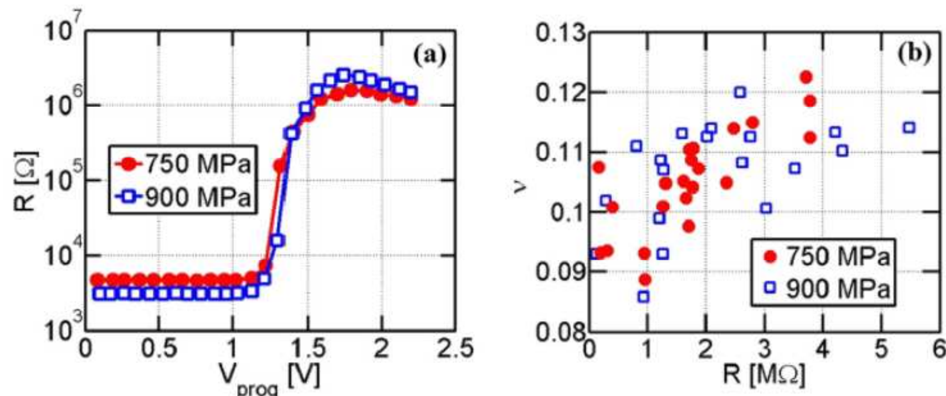

FIG. 2. (Color online) Measured resistance as a function of programming voltage Vprog (a) and drift exponent m as a function of R (b) for PCM cells with high and low compressive stress levels in the amorphous cap. The different internal stress due to stressor layers do not result in significantly different drift behaviors.

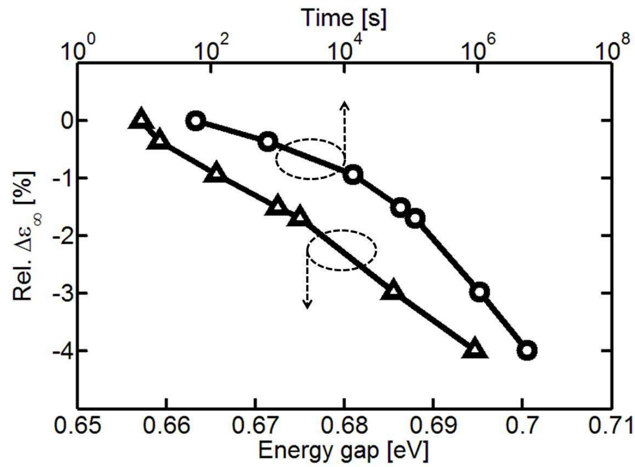

FIG. 3. Correlation between the decrease of e1 and the increase of the gap size derived from the absorption spectra analysis by using Eq. (3) (triangles). The relative decrease of e1 as a function of acquisition times (upper x-axis) is also reported (circles).

the programming curve for PCM devices with different compressive stresses in the amorphized region. To measure the programming curve, the cell was initially programmed in the set state (fully crystalline phase), then a sequence of pulses with increasing voltage V_{prog} was applied. The programming curve reports the resistance R measured after each pulse as a function of V_{prog}. The sharp increase of R at about V_{prog} = 1.3 V marks the onset of the melting region, where the applied pulse results in the formation of an amorphous region of increasing size. The resistance window slightly increases for increasing compressive stress, due to a decreasing R in the crystalline (set) state and an increasing R in the amorphous (reset) state. Fig. 2b shows the extracted drift exponent ν as a function of the programmed R for the two different stress levels. The drift exponent is about 0.1 and increases with R. The R-dependent ν was previously explained as a result of the increase of activation energy for conduction E_A with the amorphous size due to the percolation hopping in the randomly distributed energy barriers6. Both R and ν are in fact controlled by the activation energy for conduction, thus they both increase for increasing E_A due to the thicker amorphous region. Most importantly, however, no significant change of ν can be seen depending on the stress level. These results indicate that a larger compressive stress does not result in a larger tendency to drift, namely a larger ν. Therefore, our data support the picture of resistance drift dictated by SR in the amorphous volume.

3. THE SECOND PIECE: THE BANDGAP WIDENING

Furthermore, we recently demonstrated that drift is ascribed to spontaneous structural relaxation (SR) phenomena lowering the α-GST internal energy and that progressively open the size of the gap over time [11]. In particular, we have shown as the atomic rearrangements responsible for drift are related with the removal of residual resonant-like bonding in the amorphous network [12].

Fig. 3 reports the correlation plot between the relative lowering of ε_∞ and the energy gap widening over time as obtained by the optical characterization on the α-GST film considering all the acquisition times between 1 min and 173 hours. The values of the energy gap with time were obtained by Tauc model as reported in ref. [12]. Also the relative ε_∞ decrease as a function of time is reported in Fig. 3 (upper x-axis).

Since in phase change materials ε_∞ is strongly related with the orientational order of the *p*-type orbitals that directly rules the optical matrix element for ε_2, its reduction over time appears a manifestation that *p* orbitals misalignment is increasing [13,14]. In particular, a higher presence of tetrahedral Ge sites or, more in general, of defective octahedral atoms increase the angular disorder in the bonding network and lead to lower the electronic dielectric constant as reported by Caravati et al. [15]. On the contrary, resonant bonding that enhances the optical dielectric constant of the crystalline phase needs a high medium range order level where the second and higher neighbours are aligned. Thus, the decrease in ε_∞ of the amorphous phase over time can be taken as clear evidence that the medium-range order (MRO) of the amorphous network is reducing as a consequence of local distortions as such

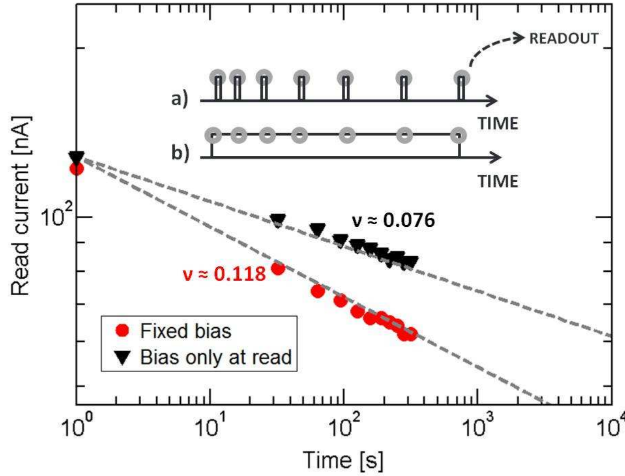

FIG. 4. Averaged measured current on 10 Kbits of PCM cells as a function of time after the reset by using the biased-only-at-read algorithm (triangles) and fixed readout bias algorithm (dots). Inset of Figure reports the sketch of the two acquisition procedures of the drift curves: a) the one supplies cells only for the readout operation and b) the one that maintains fixed the readout bias for the entire drift experiment, starting 1 s after the reset operation.

Peielrs-like distortions [16]. In particular, in order to lower the system energy it is possible that the amorphous structure distorts or breaks residual fourfold rings reminiscing the crystalline phase and present in the amorphous network, thus reducing any *p* orbital alignment. This could cause the resistance drift in the amorphous GST material.

4. THE THIRD PIECE: THE EFFECT OF ELECTRIC FIELD

In this section we show, in addition, that resistance drift in α-GST can be also controlled, or more precisely accelerated, by means of a bias voltage applied to the cell. Fig. 4 shows two typical drift measurements reporting the current decrease as a function of time after the reset programming pulse. The log-log scale is used to highlight that the current decrease follows the power law by Eq. 1 with slope ν. Experimental data of Fig. 1 correspond to the average current decrease collected by 10 Kbits of PCM cells in our 45 nm technology array [17]. In particular, the curve that more rapidly decreases (higher ν) is acquired with a fixed readout bias on the cells for the entire time of drift experiment, while the one corresponding to the slower current decrease (lower ν) is obtained biasing the same 10 Kbits cells only during the readout operation (see inset of Fig. 4). Thus, a constant applied bias is able to accelerate the drift phenomenon like an annealing process. Then, we considered our experimental finding in the Gibb's interpretative framework of SR [18] and we added the effect of a supply bias on the SR kinetics with the hypothesis of isothermal conditions.

In agreement with ref. [18] we modeled the amorphous network as an ensemble of independent TLS represented in the energy diagram of Fig. 5) where the x-axis is regarded as a general coordinate, which could be for example an atomic displacement or the bound angle orientation of an atom or a cluster of atoms. E_1, E_2 are the states of the local minimum potential, being ΔE the separation in between and E_{12} the barrier of the E_1 to E_2 transition. Here we are considering $\Delta E >> kT$. In this case the rate equation ruling the time evolution of the fractional occupancy n_1 of the state E_1 can be written as:

$$\frac{dn_1(t)}{dt} = -n_1(t) \cdot \nu_0 \cdot \exp\left(-\frac{E_{12}}{kT}\right) \tag{2}$$

where ν_0 is the frequency of attempts to jump from state E_1 to state E_2 in the time $t_0 = \frac{1}{\nu_0}$.

This approach allows to compute the increase of bias dependent activation energy $E_A(V_D)$ with time:

$$\Delta E_A(t,T,V_D) = N_{TLS} \cdot \frac{\nu \cdot kT}{1-\beta q V_D} \log\left(\frac{t}{t_0}\right) \tag{3}$$

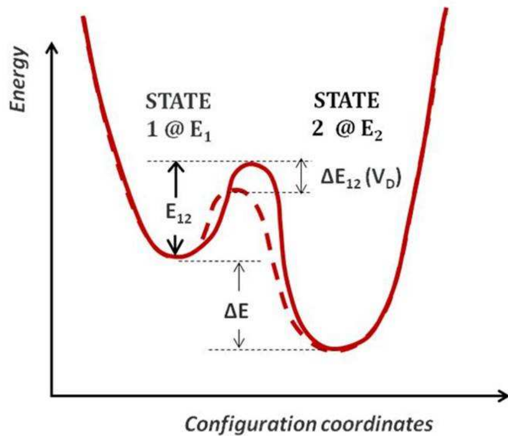

FIG. 5. Two-Level System energy diagram both in the absence of an applied bias (continuous line) and when a constant bias is applied (dashed line).

Eq. 3 can be used to simulate the current decrease with time for both $V_D = 0$ and $V_D = V_{READ}$. In fact, the current evolution can be obtained by means of the well known Arrhenius law: $I = I_0 \cdot exp[-E_{A0}+\Delta E_A(t, T, V_D)]/kT$. In particular, the value of the parameter β in Eq. 3 can be extracted by fitting the two drift trends, with $V_D = 0$ and with $V_D = 0.4$ V in Fig. 4. The so obtained simulation results are reported in Fig. 4 as dashed lines.

5. THE MISSING PIECES

The resulting picture of the *drift* phenomenon must be coherent with the experimental findings reported in the previous sections: a) mechanical stress does not seem to be responsible of SR phenomena that are inherent to chalcogenide glasses; b) a band-gap widening leading to a rearrangement of the atomic bonds occurs to explain the resistance *drift*; c) *drift* can be accelerated by means of a voltage bias applied to the cell.
However, a microscopic, atomic-like picture of the *drift* appears today missing. And some experimental findings need to be explained. For example, why the drift coefficient decreases with the programming pulse or the PCM dome as reported in Fig. 6 [19] if stress does not control ν? Are these amorphous states different form SR point-of-view? What are their differences?

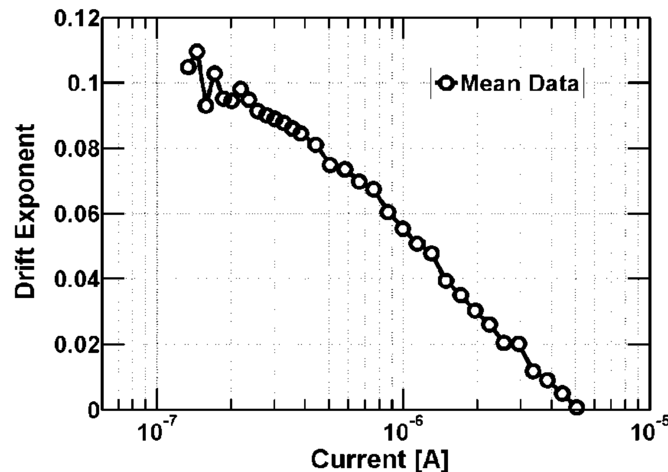

Fig. 6. Drift exponent as a function of the readout current and, then, as a function of the amorphous thickness [19].

6. CONCLUSIONS

We collected some tiles for a comprehensive picture of the drift phenomenon in PCM. Structural rearrangements phenomena seem to be the correct interpretative framework of the drift. However, further research activity, both theoretical and experimental like, is needed to complete the picture from a microscopic point of view.

REFERENCES

[1] R. Bez, IEEE International Electron Devices Meeting (IEDM) Tech. Dig., 89-92, 2009.
[2] D. Ielmini, A.L. Lacaita, and D. Mantegazza, IEEE Trans. El. Dev., 54, 2, 308-315, (2007).
[3] A. Pirovano, A. L. Lacaita, F. Pellizzer, S. A. Kostylev, A. Benvenuti, and R. Bez, IEEE Trans. Electron Devices **51**, 714 (2004).
[4] I. V. Karpov, M. Mitra, D. Kau, G. Spadini, Y. A. Kryukov, and V. G. Karpov, *J. Appl. Phys.* **102**, 124503 (2007).
[5] M. Boniardi and D. Ielmini, *Appl. Phys. Lett.* **98**, 243506 (2011).
[6] E. P. Donovan, F. Spaepen, D. Turnbull, J. M. Poate, and D. C. Jacobson, *J. Appl. Phys.* **57**, 1795 (1985).
[7] S. Roorda, W. C. Sinke, J. M. Poate, D. C. Jacobson, S. Dierker, B. S. Dennis, D. J. Eaglesham, F. Spaepen, and P. Fuoss, Phys. Rev. **B**, Condens. Matter **44**, 3702 (1991).
[8] D. B. Miracle, T. Egami, K. M. Flores and K. F. Kelton, MRS Bull. 32, 629 (2007).
[9] K. F. Kelton and F. Spaepen, Phys. Rev. **B** 30, 5516 (1984).
[10] M. Rizzi, A. Spessot, P. Fantini, and D. Ielmini, *Appl. Phys. Lett.* **99**, 223513 (2011).
[11] S. Tiwari, M. V. Fischetti, P. M. Mooney, and J. Welser, Tech. Dig. - Int. Electron Devices Meet. 1997, 939.
[12] P. Fantini, S. Brazzelli, E. Cazzini and A. Mani, *Appl. Phys. Lett.* **100**, 13505 (2012).
[13] P. Fantini, M. Ferro, A. Calderoni, and S. Brazzelli, *Appl. Phys. Lett.*, **100**, 213506 (2012).
[14] K. Shportko, S. Kremers, M. Woda, D. Lencer, J. Robertson and M. Wuttig, *Nature Mater.* **7**, 653-658 (2008).
[15] S. Caravati, M. Bernasconi and M. Parrinello, J. Phys.: Condens. Matter **22**, 315801 (2010).
[16] R. E. Peielrs, *Quantum theory of Solids* (Oxford Univ. Press, Oxford, 1956).
[17] G. Servalli, IEEE International Electron Devices Meeting (IEDM) Tech. Dig., 113-116, 2009.
[18] M. R. J. Gibbs, J. E. Evetts, and J. A. Leake, *J. Mater. Sci.* **18** 278-288 (1983).
[19] A. Calderoni, M. Ferro, D. Ventrice, P. Fantini and D. Ielmini, *Proc.* of International Memoery Workshop 2011.

Biographies

Paolo Fantini received the Laurea degree (cum laude) and the Ph.D.in physics from the University of Modena and Reggio Emilia (Italy) in 1995 and 1999, respectively. In 2000 he joined in STMicroelectronics (Agrate Brianza, Italy) in the Compact Modeling Team of the Department of Research and Development. In 2004 he became the Team Leader of the Compact Modeling Team, maintaining this position after the foundation of Numonyx (2008). Again, for Micron Technology, Inc. (Agrate Brianza, Italy) he is currently the Team Leader of the Characterization and Compact Modeling Team in Process R&D and Senior Member of the Technical Staff.
He has (co-)authored more than 80 publications in international journals and conferences covering many fields including solid-state physics, device physics, device characterization and modeling, low-frequency noise, and nonvolatile memories. He has also filed 7 patents. He served the Technical Committees of the IEEE International Electron Devices Meeting in 2009 and 2010.